



Title	Effect of periacetabular osteotomy on the distribution pattern of subchondral bone mineral density in patients with hip dysplasia
Author(s)	Shimizu, Tomohiro; Takahashi, Daisuke; Nakamura, Yumejiro et al.
Citation	Journal of orthopaedic research, 40(11), 2626-2631 https://doi.org/10.1002/jor.25284
Issue Date	2022-11
Doc URL	https://hdl.handle.net/2115/90685
Rights	© 2022. This manuscript version is made available under the CC-BY-NC-ND 4.0 license http://creativecommons.org/licenses/by-nc-nd/4.0/
Rights(URL)	https://creativecommons.org/licenses/by-nc-nd/4.0/
Type	journal article
File Information	jor.25284.pdf



1 **Effect of periacetabular osteotomy on the distribution pattern of subchondral bone mineral**
2 **density in patients with hip dysplasia**

3 Tomohiro Shimizu*, Daisuke Takahashi, Yumejiro Nakamura, Takuji Miyazaki, Shunichi
4 Yokota, Hotaka Ishizu, Norimasa Iwasaki

5 *Corresponding author

6

7 Department of Orthopaedic Surgery, Faculty of Medicine and Graduate School of Medicine,
8 Hokkaido University, Kita-15, Nish-7, Kita-ku, Sapporo 060-8638, Japan

9

10 **Corresponding author**

11 Tomohiro Shimizu, MD, PhD, Department of Orthopaedic Surgery, Faculty of Medicine and
12 Graduate School of Medicine, Hokkaido University, Kita-15, Nishi-7, Kita-ku, Sapporo 060-
13 8638, Japan. Telephone: +81-11-706-5935, Fax: +81-11-706-6054.

14 E-mail: simitom@wg8.so-net.ne.jp

15

16 **Running title:** Effect of periacetabular osteotomy

17

18 **Author contributions statement:**

19 Tomohiro Shimizu contributed to research design, data acquisition, analysis and interpretation of
20 data, and drafting of the paper; Daisuke Takahashi contributed to data acquisition and analysis
21 and interpretation of data; Yumejiro Nakamura contributed to data acquisition and analysis and
22 interpretation of data; Takuji Miyazaki contributed to data acquisition; Shunichi Yokota
23 contributed to data acquisition; Hotaka Ishizu contributed to data acquisition; Norimasa Iwasaki

24 contributed to interpretation of data. All authors have read and approved the final submitted
25 manuscript.

26

27

28 **Abstract**

29 Despite the availability of long-term follow-up data, the effect of pelvic osteotomy on the natural
30 history of osteoarthritis is not yet fully understood, partly because there is untapped potential for
31 radiographs to better describe osteoarthritis. Therefore, this study aimed to assess the distribution
32 of subchondral bone mineral density (BMD) across the acetabulum in patients with hip dysplasia
33 immediately (2 weeks) and 1 year after undergoing periacetabular osteotomy (PAO). To that end,
34 we reviewed 40 hips from 33 patients with developmental dysplasia of the hip (DDH) who
35 underwent PAO between January 2016 and July 2019 at our institution. We measured
36 subchondral BMD through the articular surface of the acetabulum using computed tomography
37 (CT) osteoabsorptiometry (OAM), dividing the distribution map into nine segments. We then
38 compared the subchondral BMD between 2 weeks and 1 year after PAO in each area. At 2 weeks
39 after PAO, the high-density area tended to be localized particularly in the lateral part of the
40 acetabulum, whereas 1 year after PAO, the high-density area moved to the central and lateral
41 parts. The percentage ratios of the subchondral BMD for the central-posterior, lateral-central, and
42 lateral-posterior areas relative to the central-central area were significantly decreased at 1 year
43 after PAO, as compared to those at 2 weeks after PAO. These findings suggest that loading was
44 altered by PAO to be more similar to physiological loading. Long follow-up observational study
45 is warranted to confirm the association between early changes in subchondral BMD by PAO and
46 joint degeneration.

47

48

49

50 **Keywords:** hip dysplasia, bone mineral density, periacetabular osteotomy

51 **Introduction**

52 Developmental dysplasia of the hip (DDH) with associated structural instability is one of the
53 more common causes of secondary osteoarthritis^{1,2}. Deficiency of the bony acetabulum results in
54 hip instability and acetabular rim overload with subsequent damage to the labrum and articular
55 cartilage³. Finite element analysis (FEA) has shown that DDH models showed stress
56 concentration in the acetabular edge and contacting femoral head, as compared to the normal hip
57 joint model⁴. As such, reducing articular cartilage contact stress by pelvic osteotomy may delay
58 the appearance or reduce the severity of osteoarthritis^{5,6}. Multiple types of pelvic osteotomies
59 have been described, with intermediate- and long-term clinical and radiographic results,
60 suggesting that these procedures can prevent the progression of DDH to secondary
61 osteoarthritis⁷⁻¹⁰. However, despite the availability of long-term follow-up data, the effect of
62 pelvic osteotomy on the natural history of osteoarthritis is not yet fully understood, partly
63 because there is untapped potential for radiographs to better describe osteoarthritis.

64 The pattern of subchondral bone density reportedly reflects the distribution of cumulative
65 stresses acting on a joint surface under actual loading conditions¹¹. As early changes in the
66 subchondral bone can predict subsequent symptoms or disease structural progression, new tools
67 may help clinicians to stratify different osteoarthritis phenotypes based on bone remodeling
68 status¹². Given this theoretical background, Müller-Gerbl et al. have developed a method of
69 computed tomography (CT) osteoabsorptiometry (CTOAM) to assess the long-term stress
70 distribution of individual joints in living subjects by measuring subchondral bone density as a
71 surrogate for cumulative stress and loading abnormalities^{11, 13}. Using this method, previous
72 studies have evaluated the stress distribution of different joints under various loading conditions,
73 from normal to pathologic or postoperative conditions¹⁴⁻¹⁸. Focusing on the hip joint, a previous

74 study reported significant differences in the severity and patterns of loading based on the severity
75 of dysplasia, as compared to the control group¹⁸. Therefore, CTOAM could detect the effect of
76 pelvic osteotomy, as the subchondral bone mineral density (BMD) changes over time after PAO
77 would be a good surrogate measure for loading changes.

78 We hypothesized that periacetabular osteotomy (PAO) would change the distribution of
79 subchondral bone density across the acetabulum. In the present study, a modified method of
80 CTOAM was employed to test this hypothesis^{19, 20}. Thus, this study aimed to assess the
81 distribution of subchondral BMD across the acetabulum in patients with DDH immediately (2
82 weeks) and 1 year after undergoing PAO.

83

84 **Methods**

85 *Subjects*

86 This study was retrospective cohort study (level of evidence, level III). This study was
87 conducted in accordance with the ethical standards of the Declaration of Helsinki and was
88 approved by our Institutional Review Board (#017-0508). A total of 41 hips from 34 patients (4
89 males and 30 females) with DDH underwent PAO between January 2016 and July 2019 at our
90 institution. This study only included 40 hips, excluding one patient who delayed rehabilitation
91 due to fracture of the posterior column. The mean age of the patients at surgery was 32.8 years
92 (range, 14–55 years), and the mean body mass index (BMI) was 23.1 kg/m² (range, 17.8–37.9
93 kg/m²) (Table 1). Surgical indications for PAO included acetabular dysplasia with a lateral center
94 of edge (CE) angle <20° and discontinuity of the Shenton's line²¹, unsuccessful 6-month
95 nonoperative treatment, age <60 years, an excellent or grade of the preoperative joint congruency
96 in abduction according to classification of joint congruency described by Yasunaga²², and no

97 pain on hip flexion and extension with the extremity held in abduction²³.

98 ***Surgery and rehabilitation***

99 All osteotomies were performed by one of four board-certified, fellowship-trained
100 orthopedic surgeons at a single institution. The type of PAO used was eccentric rotational
101 acetabular osteotomy (ERAO)²³, an improved version of rotational acetabular osteotomy²⁴. The
102 operative techniques have been described previously²³. Briefly, a 20-cm curved skin incision was
103 made 5 cm proximal to the tip of the greater trochanter. The greater trochanter was then retracted
104 proximally after completion of osteotomy at its base, with an approximate thickness of 10–15
105 mm, and the gluteus minimus and medius muscles were reflected approximately 30 mm from the
106 acetabular rim. The osteotomy site was approximately 15–20 mm or greater from the joint space
107 according to the preoperative planning. Following osteotomy of the ilium and pubis, the
108 acetabular fragment was rotated easily, wherein trimming of the inner cortex of the ilium was
109 essential for medializing the acetabular fragment. Coverage of the femoral head by the rotated
110 acetabular fragment was verified using an image intensifier before fixation of the acetabular
111 fragment with two or three polylactide screws. Afterwards, the greater trochanter was
112 repositioned and fixed with two AO cancellous screws. Postoperatively, one-third partial weight-
113 bearing was permitted with a walker after 4 weeks, one-half partial weight bearing was permitted
114 after 6 weeks, and full weight-bearing was allowed after 8 weeks. One year after PAO, the
115 patients underwent surgery to remove the two AO cancellous screws.

116 ***Clinical and radiological evaluation***

117 Clinical evaluations were performed using the Harris hip score (HHS)²⁵ and the Japanese
118 Orthopedic Association Hip-Disease Evaluation Questionnaire (JHEQ)²⁶ preoperatively and 1
119 year after PAO. Range of motion was measured by goniometry. Supine anterior–posterior (AP)

120 pelvic radiographs and CT scans were taken preoperatively, 2 weeks after PAO, and 1 year after
121 PAO (average radiation exposure per examination, 5.5 mSv). The radiographs were obtained
122 using Siebenrock's standardized technique²⁷, and the CE angle, Sharp angle, acetabular head
123 index (AHI)²⁸, and acetabular roof obliquity (ARO) were evaluated²⁹. All digital measurements
124 and calculations were performed using the Centricity™ Web-J 3.0 HD software (GE Healthcare
125 Japan, Tokyo, Japan). Measurements were performed two times with a 3-month interval by the
126 first two authors (T.S. and N.Y.), showing almost excellent intra- and inter-class correlation
127 coefficients (0.943, $P < 0.001$, and 0.873, $P < 0.001$; respectively). A high-resolution (pixel
128 matrix, 512×512) helical CT scanner (CT High Speed Advantage; GE Medical Systems,
129 Milwaukee, WI, USA) was used to obtain axial images of the bilateral hips with an intensity
130 calibration phantom (B-MAS200, Kyoto Kagaku, Kyoto, Japan). The slice thickness and interval
131 were set to 1 mm each, and the table speed was set to 1 mm/s. Imaging data were analyzed using
132 the Aquilion One image analysis system (Toshiba Medical Systems, Tokyo, Japan), and a three-
133 dimensional bone model was generated from the axial image stack. Thereafter, anterior pelvic
134 plane-based coronal views at 1-mm intervals were reconstructed using the multiplanar
135 reconstruction model.

136 To evaluate subchondral bone density, we used OsteoDens 4.0, a noncommercial
137 software developed at our institution¹⁶⁻¹⁹. The target area was the subchondral bone region of the
138 weight-bearing acetabular surface. In the coronal image, the region-of-interest was manually
139 selected to include the entire subchondral bone layer of the acetabulum in all slices, numbering
140 an average of 102.4 coronal slices (range, 92–115 slices) to capture the acetabulum. After
141 establishing the region-of-interest, we automatically measured the subchondral bone of the
142 undersurface of the acetabular at each coordinate point at 1-mm intervals in Hounsfield units

143 (HU), which is defined as the radiograph attenuation whereby water is 0 and compact bone is
144 1000 (Fig. 1). Measurement and mapping were repeated in each slice, and the data were stacked
145 to create a two-dimensional mapping image showing the distribution of subchondral bone
146 density. We then divided the acetabulum automatically into three equal parts following the front-
147 back and medial-lateral directions, and the measured target area was divided into nine regions:
148 medial anterior (MA), medial central (MC), medial posterior (MP), central anterior (CA), central
149 center (CC), central posterior (CP), lateral anterior (LA), lateral central (LC), and lateral
150 posterior (LP) (Fig. 1B). The mean bone density, corrected using the phantom (B-MAS200,
151 Kyoto Kagaku, Kyoto, Japan), was measured for each region. Additionally, to evaluate the
152 distribution, we investigated the ratios of the subchondral BMD of each area to that of the CC
153 area.

154 Furthermore, we calculated the intra- and interobserver reproducibility of the CTOAM
155 based on the five consecutive measurements and based on the measurements of the two
156 orthopedic surgeons (T.S. and N.Y.), respectively. The reliabilities between and within each
157 observer were calculated according to the intraobserver, interobserver, and residual variances
158 estimated by the analysis of variance table based on Proc Mixed in the SAS software (SAS
159 Institute, Cary, NC, USA). The intra-class correlation coefficients for intra- and interobserver
160 reproducibility were 0.86 (95% confidence interval [CI], 0.73–0.97) and 0.79 (95% CI, 0.65–
161 0.91), respectively.

162 ***Statistical analysis***

163 Paired *t*-tests with Bonferroni correction were used to compare the clinical evaluation and
164 BMD of the subchondral bone preoperatively, 2 weeks after PAO, and 1 year after PAO.
165 Correlations between BMI and subchondral BMD were performed using Pearson's product–

166 moment correlation coefficient. All statistical analyses were performed using the IBM SPSS
167 version software (SPSS Inc., Chicago, IL, USA), and statistical significance was set at $p < 0.05$.

168

169 **Results**

170 *Demographic characteristics, clinical score, and radiographic parameters*

171 Table 1 summarizes the longitudinal clinical scores and radiographic parameters in this
172 study. Although internal rotation was limited at 1 year postoperatively ($P = 0.005$), clinical
173 scores, including the HHS and JHEQ, were significantly improved, as compared to those
174 preoperatively ($P < 0.001$). The mean CE angle and mean AHI increased, whereas the mean
175 Sharp angle and mean ARO decreased significantly from the preoperative to postoperative values
176 (all $P < 0.001$).

177 *Analysis of patients treated with PAO*

178 At 2 weeks after PAO (immediately after surgery), the high-density area tended to be
179 localized in the lateral part of the acetabulum (Fig. 2A), whereas at 1 year after PAO, the high-
180 density area moved to the central and lateral parts. In the quantitative evaluation of the
181 subchondral BMD calibrated according to the phantom, mean BMD values in the medial, CA,
182 and CC areas at 1 year after PAO were significantly higher than those at 2 weeks after PAO (Fig.
183 2B). To evaluate subchondral BMD distribution, we investigated the ratios of the subchondral
184 BMD of each area to that of the CC area (Fig. 2C). The percentage ratios of the subchondral
185 BMD for the CP, LC, and LP areas relative to the CC area were significantly decreased at 1 year
186 after PAO, as compared to those at 2 weeks after PAO. No significant associations between BMI
187 and subchondral BMD were observed (Supplemental Table 1).

188

189 **Discussion**

190 Clinically, PAO has been reported to be an effective treatment for early osteoarthritis in young or
191 active patients with DDH³⁰⁻³². Moreover, this study showed the significant improvement of HHS
192 and patient-based clinical outcomes (JHEQ) from preoperative to 1 year after surgery. Despite
193 this, although simulation studies using finite or discrete element analysis showed alterations of
194 contact stress by PAO^{4,33}, findings on changes in the mechanical environment due to PAO have
195 not yet been fully clarified. In this study using CTOAM, we found that PAO shifted the area with
196 the highest subchondral BMD from the lateral to the central region and reduced the ratio of
197 subchondral BMD in the CP, LC, and LP areas relative to that in the CC area, thus confirming
198 our hypothesis.

199 The finding that the subchondral BMD on the lateral side tended to be higher than that on
200 the medial and center areas at 2 weeks after PAO showed a similar tendency to a previously
201 described study on severe dysplasia subjects¹⁸, suggesting that CTOAM data at 2 weeks after
202 PAO may reflect the preoperative mechanical environment. Moreover, the finding that the
203 subchondral BMD in the central area tended to be higher than that in other areas at 1 year after
204 PAO showed a similar tendency to the control subjects ($25^\circ < \text{CE angle} < 35^\circ$) of that same
205 study¹⁸. Although one of the main limitations of the current study was the indirect measure of
206 mechanical stress with acetabular subchondral BMD using CTOAM, we believe that these
207 findings suggest that loading was altered by PAO to be more similar to physiological loading.

208 Contrary to our expectations and previous reports using FEA^{34,35}, this study showed that
209 the absolute subchondral BMD in the medial, CA, and CC areas increased significantly from 2
210 weeks to 1 year after PAO. Since PAO transfers the medial part, which is considered to be a
211 lower mechanical stress area, to the central area, it is possible that the subchondral BMD in the

212 medial and central areas were relatively low at 2 weeks after PAO. Furthermore, it is possible
213 that this finding may have been affected by the limitation of weight-bearing immediately after
214 PAO. However, since this study was only a 1-year longitudinal follow-up study, a longer follow-
215 up period is necessary to address whether the increase in subchondral BMD from 2 weeks to 1
216 year after PAO would affect future joint degeneration.

217 Despite these findings, this study had a few limitations. First, we could not directly
218 measure the contact stress pressure and stress distribution patterns in the live patients' hips.
219 However, the measurements of BMD were more clinically accessible. Second, although we
220 performed fixation of the acetabular fragment with two or three polylactide screws and compared
221 the CT data on the same setting between 2 weeks and 1 year after PAO, the artifact from the
222 screws could have affected BMD distribution in this setting. Third, postoperative alterations in
223 the pattern of subchondral bone mineralization may depend not only on the biomechanical
224 effects of PAO but also on the individual loading conditions. To clarify this point, we should
225 perform further analysis based on CT data from more patients treated with PAO. Fourth, this was
226 a short follow-up observational study. Although we targeted the early changes in the subchondral
227 bone during PAO, a longer follow-up study is required to understand the association between
228 subchondral BMD and joint degeneration. Finally, because reductions in vascular supply are
229 associated with bone loss³⁶, BMD may also depend on the vascularity of the acetabular fragment.
230 As this study did not investigate the vascularity of the acetabular fragment, further studies should
231 address this concern in the future.

232 In conclusion, the findings of this study using the CTOAM method suggest that loading
233 was altered by PAO to be more similar to physiological loading. Long follow-up observational

234 studies should be performed to confirm the association between early changes in subchondral
235 BMD by PAO and joint degeneration.

236

237 **Acknowledgements**

238 We would like to thank Editage (www.editage.com) for English language editing and manuscript
239 revision.

240 Conflicts of Interest: The authors declare that they have no conflict of interest.

241 Grant sponsor: This work was supported by the Japan Society for the Promotion of Science
242 (JSPS) Grants-in-Aid for Scientific Research (KAKENHI) (Grant Number: 20K17984).

243

244 **References**

- 245 1. Aronson J. 1986. Osteoarthritis of the young adult hip: etiology and treatment. Instr
246 Course Lect 35: 119-128.
- 247 2. Harris WH. 1986. Etiology of osteoarthritis of the hip. Clin Orthop Relat Res: 20-33.
- 248 3. Klaue K, Durnin CW, Ganz R. 1991. The acetabular rim syndrome. A clinical presentation
249 of dysplasia of the hip. J Bone Joint Surg Br 73: 423-429.
- 250 4. Zhao X, Chosa E, Totoribe K, et al. 2010. Effect of periacetabular osteotomy for
251 acetabular dysplasia clarified by three-dimensional finite element analysis. J Orthop Sci 15: 632-
252 640.
- 253 5. Poss R. 1984. The role of osteotomy in the treatment of osteoarthritis of the hip. J Bone
254 Joint Surg Am 66: 144-151.
- 255 6. Millis MB, Murphy SB, Poss R. 1996. Osteotomies about the hip for the prevention and
256 treatment of osteoarthrosis. Instr Course Lect 45: 209-226.
- 257 7. van Hellemond GG, Sonneveld H, Schreuder MH, et al. 2005. Triple osteotomy of the
258 pelvis for acetabular dysplasia: results at a mean follow-up of 15 years. J Bone Joint Surg Br 87:
259 911-915.
- 260 8. Steppacher SD, Tannast M, Ganz R, et al. 2008. Mean 20-year followup of Bernese
261 periacetabular osteotomy. Clin Orthop Relat Res 466: 1633-1644.
- 262 9. Kotz R, Chiari C, Hofstaetter JG, et al. 2009. Long-term experience with Chiari's
263 osteotomy. Clin Orthop Relat Res 467: 2215-2220.
- 264 10. Kaneuji A, Sugimori T, Ichiseki T, et al. 2015. Rotational Acetabular Osteotomy for
265 Osteoarthritis with Acetabular Dysplasia: Conversion Rate to Total Hip Arthroplasty within
266 Twenty Years and Osteoarthritis Progression After a Minimum of Twenty Years. J Bone Joint

- 267 Surg Am 97: 726-732.
- 268 11. Muller-Gerbl M, Putz R, Hodapp N, et al. 1989. Computed tomography-
269 osteoabsorptiometry for assessing the density distribution of subchondral bone as a measure of
270 long-term mechanical adaptation in individual joints. Skeletal Radiol 18: 507-512.
- 271 12. Funck-Brentano T, Cohen-Solal M. 2015. Subchondral bone and osteoarthritis. Curr Opin
272 Rheumatol 27: 420-426.
- 273 13. Muller-Gerbl M, Putz R, Hodapp NH, et al. 1990. Computed tomography-
274 osteoabooprptiometry: a method of assessing the mechanical condition of the major joints in a
275 living subject. Clin Biomech (Bristol, Avon) 5: 193-198.
- 276 14. Momma D, Iwasaki N, Oizumi N, et al. 2011. Long-term stress distribution patterns
277 across the elbow joint in baseball players assessed by computed tomography
278 osteoabsorptiometry. Am J Sports Med 39: 336-341.
- 279 15. Makabe H, Iwasaki N, Kamishima T, et al. 2011. Computed tomography
280 osteoabsorptiometry alterations in stress distribution patterns through the wrist after radial
281 shortening osteotomy for Kienbock disease. J Hand Surg Am 36: 1158-1164.
- 282 16. Nishida K, Iwasaki N, Fujisaki K, et al. 2012. Distribution of bone mineral density at
283 osteochondral donor sites in the patellofemoral joint among baseball players and controls. Am J
284 Sports Med 40: 909-914.
- 285 17. Shimizu T, Iwasaki N, Nishida K, et al. 2012. Glenoid stress distribution in baseball
286 players using computed tomography osteoabsorptiometry: a pilot study. Clin Orthop Relat Res
287 470: 1534-1539.
- 288 18. Irie T, Takahashi D, Asano T, et al. 2018. Is There an Association Between Borderline-to-
289 mild Dysplasia and Hip Osteoarthritis? Analysis of CT Osteoabsorptiometry. Clin Orthop Relat

- 290 Res 476: 1455-1465.
- 291 19. Iwasaki N, Minami A, Miyazawa T, et al. 2000. Force distribution through the wrist joint
292 in patients with different stages of Kienbock's disease: using computed tomography
293 osteoabsorptiometry. *J Hand Surg Am* 25: 870-876.
- 294 20. Oizumi N, Suenaga N, Minami A, et al. 2003. Stress distribution patterns at the
295 coracoacromial arch in rotator cuff tear measured by computed tomography osteoabsorptiometry.
296 *J Orthop Res* 21: 393-398.
- 297 21. Jones DH. 2010. Shenton's line. *J Bone Joint Surg Br* 92: 1312-1315.
- 298 22. Yasunaga Y, Ikuta Y, Kanazawa T, et al. 2001. The state of the articular cartilage at the
299 time of surgery as an indication for rotational acetabular osteotomy. *J Bone Joint Surg Br* 83:
300 1001-1004.
- 301 23. Hasegawa Y, Iwase T, Kitamura S, et al. 2002. Eccentric rotational acetabular osteotomy
302 for acetabular dysplasia: follow-up of one hundred and thirty-two hips for five to ten years. *J*
303 *Bone Joint Surg Am* 84: 404-410.
- 304 24. Ninomiya S, Tagawa H. 1984. Rotational acetabular osteotomy for the dysplastic hip. *J*
305 *Bone Joint Surg Am* 66: 430-436.
- 306 25. Harris WH. 1969. Traumatic arthritis of the hip after dislocation and acetabular fractures:
307 treatment by mold arthroplasty. An end-result study using a new method of result evaluation. *J*
308 *Bone Joint Surg Am* 51 :737-755.
- 309 26. Matsumoto T, Kaneuji A, Hiejima Y, et al. 2012. Japanese Orthopaedic Association Hip
310 Disease Evaluation Questionnaire (JHEQ): a patient-based evaluation tool for hip-joint disease.
311 The Subcommittee on Hip Disease Evaluation of the Clinical Outcome Committee of the
312 Japanese Orthopaedic Association. *J Orthop Sci* 17: 25-38.

- 313 27. Siebenrock KA, Schoeniger R, Ganz R. 2003. Anterior femoro-acetabular impingement
314 due to acetabular retroversion. Treatment with periacetabular osteotomy. *J Bone Joint Surg Am*
315 85: 278-286.
- 316 28. Heyman CH, Herndon CH. 1950. Legg-Perthes disease; a method for the measurement of
317 the roentgenographic result. *J Bone Joint Surg Am* 32 A: 767-778.
- 318 29. Massie WK, Howorth MB. 1950. Congenital dislocation of the hip. Part I. Method of
319 grading results. *J Bone Joint Surg Am* 32-A: 519-531.
- 320 30. Janssen D, Kalchschmidt K, Katthagen BD. 2009. Triple pelvic osteotomy as treatment for
321 osteoarthritis secondary to developmental dysplasia of the hip. *Int Orthop* 33: 1555-1559.
- 322 31. Hasegawa Y, Iwase T, Kitamura S, et al. 2014. Eccentric rotational acetabular osteotomy
323 for acetabular dysplasia and osteoarthritis: follow-up at a mean duration of twenty years. *J Bone*
324 *Joint Surg Am* 96: 1975-1982.
- 325 32. Yasunaga Y, Ochi M, Yamasaki T, et al. 2016. Rotational Acetabular Osteotomy for Pre-
326 and Early Osteoarthritis Secondary to Dysplasia Provides Durable Results at 20 Years. *Clin*
327 *Orthop Relat Res* 474: 2145-2153.
- 328 33. Thomas-Aitken HD, Goetz JE, Dibbern KN, et al. 2019. Patient Age and Hip Morphology
329 Alter Joint Mechanics in Computational Models of Patients With Hip Dysplasia. *Clin Orthop*
330 *Relat Res* 477: 1235-1245.
- 331 34. Ike H, Inaba Y, Kobayashi N, et al. 2015. Effects of rotational acetabular osteotomy on the
332 mechanical stress within the hip joint in patients with developmental dysplasia of the hip: a
333 subject-specific finite element analysis. *Bone Joint J* 97-B: 492-497.
- 334 35. Abraham CL, Knight SJ, Peters CL, et al. 2017. Patient-specific chondrolabral contact
335 mechanics in patients with acetabular dysplasia following treatment with peri-acetabular

336 osteotomy. *Osteoarthritis Cartilage* 25: 676-684.

337 36. Marenzana M, Arnett TR. 2013. The Key Role of the Blood Supply to Bone. *Bone Res* 1:

338 203-215.

339

340

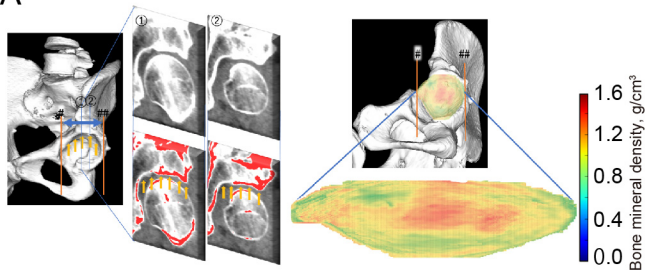
341 **Figure legends**

342 **Fig. 1.** (A) The image shows how the subchondral bone region of the acetabulum was identified
343 automatically using the customized software. In each coronal slice, we measured the Hounsfield
344 units of radiograph absorption in the subchondral bone at each coordinate point in 1-mm
345 intervals. For quantitative analysis, the distribution pattern is represented as a surface-mapping
346 image depicted by a color scale. (B) The image shows segments used for quantitative analysis of
347 the bone density mapping data for the acetabulum.

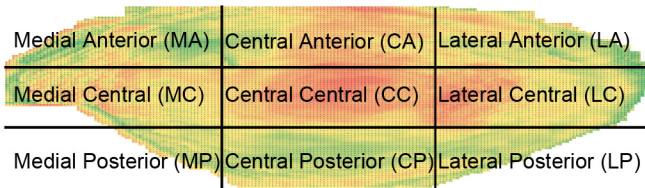
348 **Fig. 2.** (A) The images show the distribution of bone density values across the articular surface
349 of the acetabulum at 2 weeks and 1 year after periacetabular osteotomy. (B) Comparisons of the
350 subchondral bone mineral density between 2 weeks and 1 year after periacetabular osteotomy in
351 each area. (C) Comparisons of the percentage ratio of each area relative to the subchondral bone
352 mineral density in the central center area between 2 weeks and 1 year after periacetabular
353 osteotomy. Data are presented as means \pm standard deviation. Asterisks indicate $P < 0.05$.

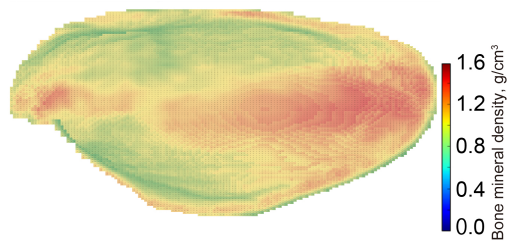
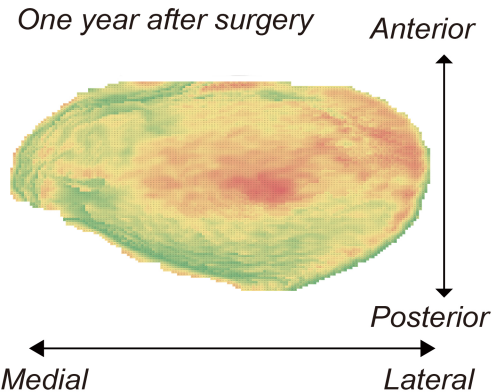
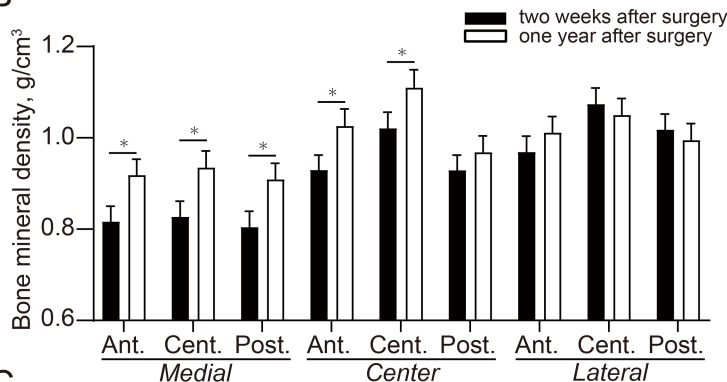
354
355
356
357
358

A



B



A*Two weeks after surgery**One year after surgery***B****C**